SHRINKAGE EIGENSTRESSES AND HARDENING OF CONCRETE

P. Paulini, University Innsbruck, Institute of Construction and Material Science, Austria

ABSTRACT

Hardening processes are always accompanied by eigenstresses. Thermal hardening reactions from molten states as well as chemical hardening reactions occur along adiabatic paths with irreversible changes of state. During hardening a bonding energy is supplied to the system and a reverse exothermic energy is released from the reacting system. Isotropic material hardening can be defined according to the specific volume strain energy based on the shrinkage volume.

The hydration of cement is accompanied by significant chemical volume shrinkage. The volume change of hydrating cement or concrete can be measured with buoyancy methods. Not only the chemical composition but also the potential of chemical shrinkage of cement is influenced by the early reaction (admixtures, temperature etc.) and by the fineness of the cement. An extrapolation to final values of chemical shrinkage of cements requires measurement periods of at least 10 to 14 days.

Ultrasonic velocity data permit access to increasing stiffness properties and can be obtained in simultaneously to buoyancy weighing measurements. The Poisson ratio, which changes from 0.5 in the fluid state towards its elastic final value, is a basic indicator for hardening.

1 INTRODUCTION

Material hardening is a process in which an energy transfer occurs in the system under consideration. Basic types of hardening are thermal setting and chemical hardening. Both processes include a supply of bond energy to the system and a loss of heat from the system. Both processes are also accompanied by volume shrinkage. In fluid states the Poisson ratio is 0.5 and both shear and Young modules become zero. Hardening reactions start from a fluid state along a path with declining Poisson ratios and raising stiffness. Therefore, hardening processes are recorded quite well by the stiffness gain and/or by the change of reaction energies.

Extensive studies have been performed by many researchers on the hardening and hydration of cement pastes and concrete [Pow48, Ver68, Byf80]. The hardening process is coupled with the kinetics of the cement hydration. Usually, it is not possible to measure the energies of cement hydration directly. Adiabatic and isothermal calorimetry were used for cement pastes [Tap59] and concrete [Des95]. Calorimetry uses the temperature change of a sample in an appropriate calorimeter and calculates with a constant heat capacity for the heat of hydration.

Volumetric measurements have been applied to cement hydration [Gei82, Pau92] to obtain chemical shrinkage of cement. The kinetic rates of both methods coincide broadly, except for certain cement types in the early hydration stage. Type II and III cements blended with fly ash, blast furnace slag or with silica fume added may lead to volume swelling during the initial reaction. The early swelling reaction can be caused by the setting time of cement, if a through solution process is considered (Fig.2) [Pau94].

In civil engineering, the evolution of stiffness and mechanical properties of concrete are of high importance. Studies have been performed using ultrasonic wave techniques for hydrated cement paste (HCP) [Bou96] and for concrete [Pop90]. Concrete is a dispersive material were the wave velocity depends on the frequency. Pulse velocity increases with the age of the concrete and will be reduced by humidity. Higher differences between dynamic and static Young modules occur in the early stage of hydration. This is caused by the relaxation of pore water pressure under static load which is prevented by short dynamic loads. Kinetic studies on HCP with simultaneous longitudinal and transversal waves have shown a linear increase of dynamic Young modules respective to the degree of hydration [Bou96].

2 SHRINKAGE VOLUME OF HYDRATED CEMENT PASTE

Usually, structural and mechanical properties of HCP and concrete are related to the degree of hydration, which is defined as the amount of hydrated cement as a fraction of the total. Other definitions of the degree of hydration α found in literature are

$$\alpha(t) = \frac{Q(t)}{Q_{Hy}} = \frac{V_{cs}(t)}{V_{cs,u}} \tag{2.1}$$

Q_{Hy} denotes the total heat of hydration and $V_{cs,u}$ the ultimate chemical shrinkage volume of cement. The time dependent quantities $Q(t)$, $V_{cs}(t)$ are assumed to change linearly with the mass of reacted cement. Then, the volume fractions of not reacted cement, capillary pores; gel pores and C-S-H gel in HCP become simple linear relations of the degree of hydration (Fig.1).

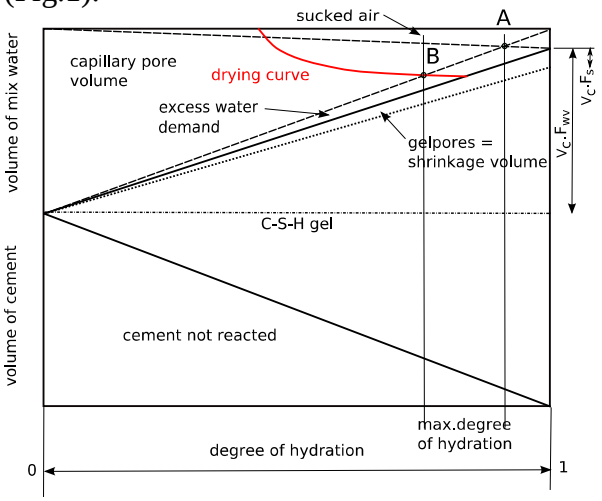

Fig. 2.1 Volume fractions of HCP vs. degree of hydration

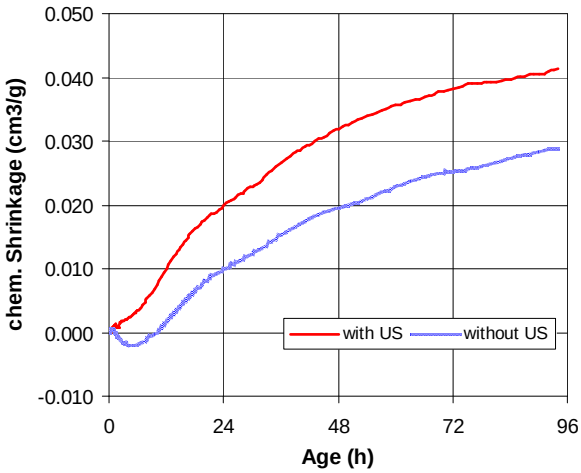

Fig. 2.2 Chemical shrinkage data of HCP CEM I 42.5N HS + 30% FA with and without ultrasonic exitation

The volumetric water-demand factor F_{wv}, the mass water-demand factor F_{wm}, the shrinkage factor F_s and the ultimate chemical shrinkage volume $V_{cs,u}$ were calculated by stoichiometrical calculation with clinker phase fractions [Pau92]:

$$F_{wv} = V_w / V_c = 0.7422 \cdot [C_3S] + 0.6874 \cdot [C_2S] + 1.2023 \cdot [C_3A] + 1.3754 \cdot [C_4AF] \quad (2.2)$$

$$F_{wm} = W / C = 0.2367 \cdot [C_3S] + 0.2092 \cdot [C_2S] + 0.40 \cdot [C_3A] + 0.3619 \cdot [C_4AF] \quad (2.3)$$

$$F_s = V_s / V_c = -(0.2243 \cdot [C_3S] + 0.1909 \cdot [C_2S] + 0.4455 \cdot [C_3A] + 0.3071 \cdot [C_4AF]) \quad (2.4)$$

$$V_{cs,u} = V_s / C = -(0.0532 \cdot [C_3S] + 0.04 \cdot [C_2S] + 0.1785 \cdot [C_3A] + 0.1113 \cdot [C_4AF]) \ (\mathrm{cm^3/g}) \quad (2.5)$$

V_w, V_c, and V_s are the volumes of chemical bound water, cement and shrinkage volume and W the mass of bound water of the hydrated cement mass C. For full hydration, an excess water volume in the mix of at least V_{cs} is required. During hydration, the volume shrinkage produces a negative pressure in the pore water, sucking it towards the mass centre and drying out free surface areas. When free surfaces are adjacent to the ambient, air will be sucked into the pores. Therefore, lean mixes with a w/c-ratio smaller than appr. 0.38 cannot hydrate totally (point A in Fig. 2.1). A further reduction of the maximum degree of hydration occurs when considering evaporation loss (point B). The volumetric water-demand factor varies in small ranges for cements $0.808 < F_{wv} < 0.827$; also absolute values of ultimate chemical shrinkage were calculated in narrow ranges $0.0577 < V_{cs,u} < 0.0699$ $\mathrm{cm^3/g}$. It should be emphasized that measured absolute values $V_{cs,u}$ were found much higher than the ones by stoichiometrical calculation which reached up to 0.1 $\mathrm{cm^3/g}$ for e.g. micro-cements.

The calculation of capillary pore volume, gel pore volume and C-S-H-gel volume can easily be performed based on above volume factors assuming linear relations to the degree of hydration. The latter can be obtained from kinetic hydration data using Eq. (2.1). The most important value for a hydraulic binder in terms of strength capacity is the ultimate shrinkage volume $V_{cs,u}$. This value is not just influenced by the chemical composition and the finess of the binder, but also curing temperatures, concrete admixtures and fine particles can affect the final shrinkage substantially. Especially early hydration can vary in a wide range, whereas the long term kinetic is determined by mean capillary pore sizes. A useful approach to obtain the ultimate shrinkage volume of cement is to perform long term buoyancy weighing during 10 to 14 days. Under such conditions, evaporation is avoided and maximal hydration can occur. The final degree of hydration is obtained by extrapolation of the decay reaction. This starts on the third or fourth day and after the main reaction (acceleration period) has settled. Either Sideris hydration equation (2.6) [Sid93] or Eq. (2.7) can be used for a least square analysis to identify the three unknown function parameters.

Sideris hydration equation:
$$V_{cs}(t) = V_{cs,u} \cdot \left(1 - \frac{k}{t^n}\right) \quad (2.6)$$

Exponential hydration equation:
$$V_{cs}(t) = V_{cs,u} \cdot exp\left(\frac{-k}{t^n}\right) \quad (2.7)$$

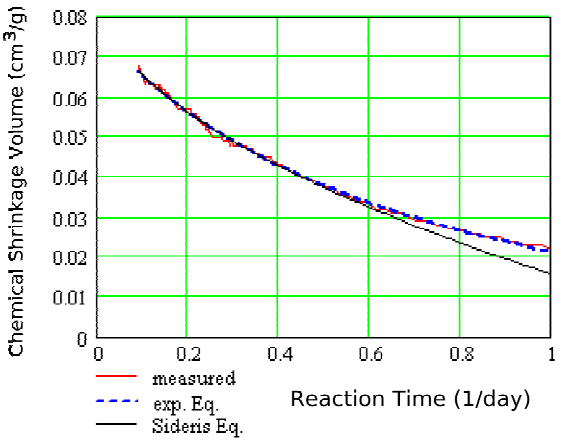

Fig. 2.3 Fit of chemical shrinkage data with two different hydration equations (Vcs,u = 0.080 / 0.087).

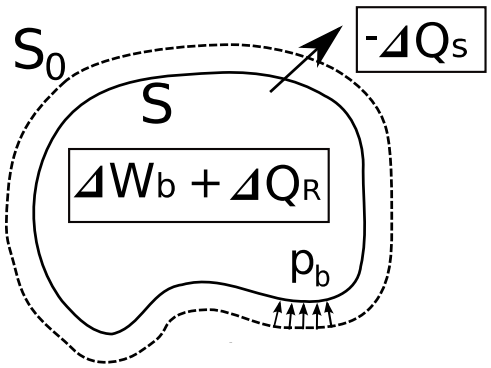

Fig. 2.4 Hardening system S_0 with bonding pressure p_b.

3 EIGENSTRESS, BOND ENERGY AND TENSILE STRENGTH

Material hardening is a process in which bond energy is supplied to the system. For reversible temperature setting processes, the bond energy ΔW_b and the heat energy leaving the system Q_s are equal energies opposing each other (ΔW_b=-ΔQ_s). Chemical hardening reactions occur along a path towards a minimum of free energy. The change of Gibbs free energy is defined as (Fig. 2.4)

$$\Delta G = -(\Delta W_b + \Delta Q_R) \tag{3.1}$$

The bond energy ΔW_b can be regarded as the result of an inner eigenstress p_b acting on the system volume. The heat of reaction ΔQ_R and the bond energy are positive for hardening reactions. This means all hardening processes are accompanied by negative volume changes (shrinkage), which holds true except for a few materials (ice formation, antimony..). The specific volume change V_s is expressed as

$$V_s = \frac{\Delta V}{V_0} = I_1(\varepsilon_{ij}) = \frac{\sigma_m}{K} = \frac{p_b}{K} \tag{3.2}$$

V_0 denotes the initial volume in the system S_0, I_1 the first strain invariant, K the bulk modulus and σ_m the mean stress. The mean stress is regarded as an inner bonding eigenstress p_b acting between atoms or molecules and responsible for material hardening. From this point of view, the eigenstress can also count for a uniform material tensile strength, which must be overruled by external stress for failure to occur in tension stress states.

The elastic modules characterize the linear stress-strain relation of a material for a specific loading test case. Only two of the six constants *E, K, G, M, λ, ν* are necessary to describe the missing material constants. Conversion tables between elastic constants are found in textbooks or at http://en.wikipedia.org/wiki/Elastic_modulus [revised on Feb. 2010]. It is rather unlikely that relations between six material constants hold true for all types of bonds (ionic, atomic, metallic and polar) and for all kind of different materials. It is much more likely that the modules *E, K, G, M, λ* are related to the strain field of the specific test conditions and that only one stiffness constant exists as an isotropic material stiffness. Assuming that the Poisson ratio ν and the Lamé constant λ are independent of each other, the conversion formulas for the other elastic modules are given by Eq. (3.3) – (3.6).

Young´s modulus $$E = \lambda \cdot \frac{(1+\nu)\cdot(1-2\cdot\nu)}{\nu} \tag{3.3}$$

Shear modulus $$G = \lambda \cdot \frac{1-2\cdot\nu}{2\cdot\nu} \tag{3.4}$$

Bulk modulus $$K = \lambda \cdot \frac{1+\nu}{3\cdot\nu} \tag{3.5}$$

P-wave modulus $$M = \lambda \cdot \frac{1-\nu}{\nu} \tag{3.6}$$

The relative modules are obtained by dividing Eq. (3.3) – (3.6) with λ. Their relations vs. the Poisson ratio are shown in Fig.3.1. Obviously for $\nu \rightarrow 0.5$ relative bulk and P-wave modules move towards one, while Young´s and shear modules tend towards zero. Hence, a hardening reaction starting from a fluid state (ν=0.5) can be described by recording the stiffness gain or the decay of Poisson´s ratio. Usually, ultrasonic wave techniques are used for this purpose.

For further considerations, we make a basic assumption about Lamé´s constant. It is assumed that λ is independent on the state of hardening and is therefore regarded as a hydrostatic material stiffness constant in the fluid state. The increase of the other stiffness constants *E, G, K* and *M* during hardening is attributed entirely to the decay of the Poisson´s ratio and the volume shrinkage. This assumption allows a description of bond energy and tensile strength. Poisson ratios less than 0.1 (diamond) are not achieved in bulk materials.

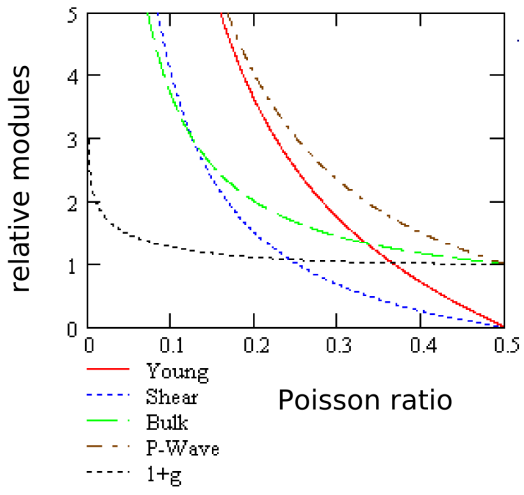

Fig. 3.1 Relative modules to λ vs. Poisson ratio.

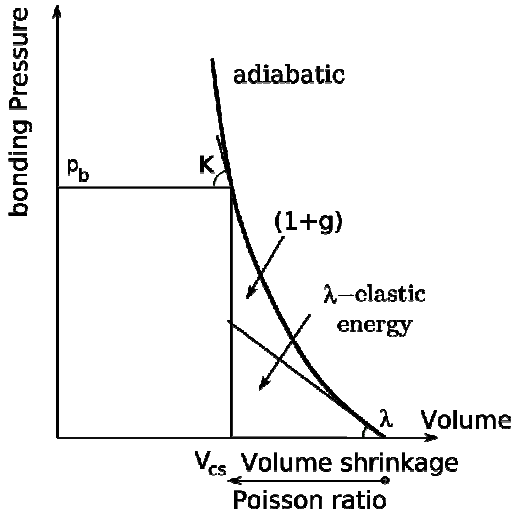

Fig. 3.2 Adiabatic shrinkage hardening.

Tensile strength f_t is defined as the specific bond energy w_b supplied to the system. Using (3.2) and (3.5) specific bond energy is expressed by the integral over the shrinkage volume (Fig.3.2).

$$W_b = -\int p_b \cdot dV = -\int \lambda \frac{1+\nu}{3 \cdot \nu} \cdot V_s \cdot dV \tag{3.7}$$

Performing the integration from an initial fluid state V_0 to the final hardened state V, we receive the tensile strength as the product of the elastic strain energy with a gain function (Eq.3.8). The gain function (1+g) rises slowly in relation to the Poisson ratio (Fig.3.1) and can be omitted for approximate calculations.

$$f_t = w_b = \frac{\lambda \cdot V_s^{\,2}}{2} \cdot (1+g) = \frac{\lambda \cdot V_s^{\,2}}{2} \cdot \left[\frac{1}{3} \cdot \left(2 \cdot \nu_{el} - ln(\nu_{el}) + 1.307 \right) \right] \tag{3.8}$$

Eq. (3.8) has been applied for a wide range of materials with reasonable tensile strength results for brittle materials. For plastic materials Eq.(3.8) represents the yield stress not accounting for the influence of strain hardening [Pau10]. Table 3.1 shows some approximate model results for totally hydrated HCP and concrete. Lamé´s constant for HCP was estimated at 7 GPa, while the w/c-ratio was assumed to be 0.38. For HCP 1420 kg/m^3 cement and for concrete 300 kg/m^3 cement were used in the calculation. Hence, the strong influence of the ultimate shrinkage volume $V_{cs,u}$ on the tensile strength is demonstrated.

Table 3.1 Model values of tensile strength for HCP and concrete

$V_{cs,u}$ (cm^3/g)	specific V_s --	f_t HPC (MPa)	f_t Concrete (MPa)	w/c limit
0.05	0.071	17.6	3.8	0.35
0.06	0.085	25.4	5.5	0.37
0.07	0.099	34.6	7.5	0.39
0.08	0.114	45.2	9.8	0.41

4 POROSITY AND WATER-CEMENT RATIO

The influence of the w/c-ratio on the strength of HCP and concrete has been studied in many reports. Capillary pore space reduces the strength f_0 of a zero-porosity material. Well known strength theories of Ryshkewitch, Balshin or Hasselman deal with the problem for general porous materials and were also used for HCP [Nie93]. He found that Balshin´s relation can be applied best for HCP with a zero-porosity compression strength of 450 MPa. Powers introduced the gel space ratio r as a volume fraction of the CSH-gel to that of CSH-gel plus capillary pore space. He found the compressive strength of concrete to be $234.r^3$ MPa [Pow58].

It has been shown that tensile strength of HCP strongly depends on the shrinkage volume (Eq. 15) and will develop differently for each cement type. By separating the influences, tensile strength can be expressed as a product of a hydration term and a porosity term. The strength loss due to capillary porosity P can be considered using the Hasselman relation (4.1) where f_0 represents the strength for zero-porosity material. Zero-porosity is not possible in HCP because an excess water volume is necessary for hydration (Fig.1). Lean mixes can not hydrate totally below a limiting w/c-ratio (Fig.2.1 point A). The limiting w/c ratio is obtained with Eq. (4.2) for ambient air conditions and some values are listed in the last column of Table 2.1. For ambient water conditions the factor 2 in Eq. (4.2) is replaced by 1. The reference tensile strength f_0 for the lowest possible porosity in HCP is obtained by calculating with Eq. (3.8).

Capillary porosities in HCP and concrete are functions of the degree of hydration α and the water/cement ratio wc. They can be calculated for HCP (4.3) and concrete (4.4) based on the volumetric water demand factor F_{wv} and the densities ρ. Fig.4.1 shows a diagram of capillary porosities for totally hydrated concrete. In (4.1) it is assumed that zero-strength porosity $P(0)$ occur for $\alpha = 0$. The Hasselman relative strength function of HCP is shown in Fig.4.2.

$$f(P) = f_0 \cdot \left(1 - \frac{P(\alpha)}{P(0)}\right) \tag{4.1}$$

$$wc_{\lim} = F_{wm} + 2 \cdot V_{cs,u} \cdot (cm^3 / g) \tag{4.2}$$

$$P_{HCP}(\alpha) = \frac{\rho_c \cdot wc - \alpha \cdot F_{wv} \cdot \rho_w}{\rho_c \cdot wc + \rho_w} \tag{4.3}$$

$$P_{Con}(\alpha) = C \cdot \left(\frac{\rho_c \cdot wc - \alpha \cdot F_{wv} \cdot \rho_w}{\rho_c \cdot \rho_w}\right) \tag{4.4}$$

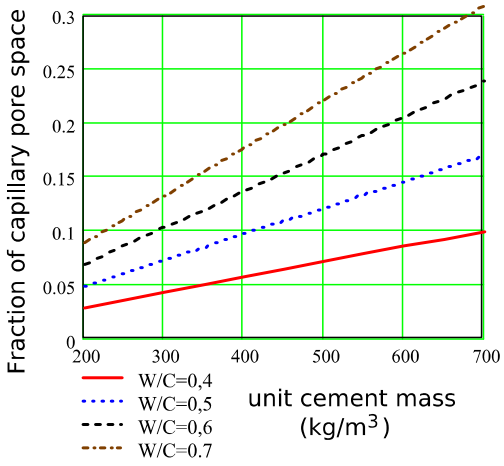

Fig. 4.1 Capillary pore volume of totally hydrated concrete vs. cement amount.

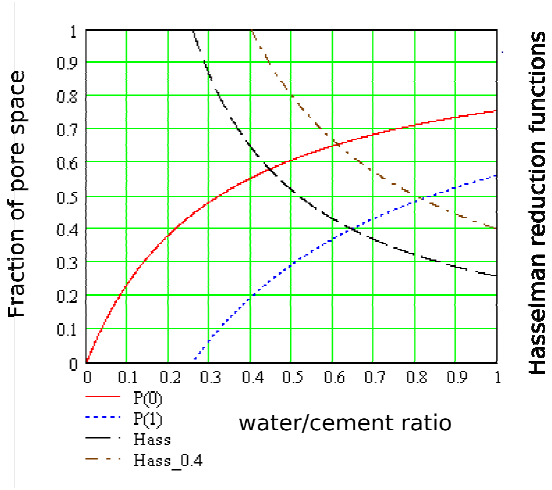

Fig. 4.2 Capillary pore space and Hasselman relative strength function for HCP.

5 STIFFNESS FORMATION

Stiffness growth of concrete at early age is determined by the hardening of HCP. A major difference between statically and dynamically measured Poisson ratios of early age concrete has been observed [Byf90]. This has been attributed to the strong relaxation of static stresses in early age concrete which can not occur in short-term dynamic measurements with ultrasound. Dynamic measurements of HCP and mortar have shown a continuous decrease in Poisson's ratio and a linear increase of Young´s modulus with respect to the degree of hydration [Bou96]. During these tests simultaneous measurements of longitudinal and transversal velocities were performed by a computer controlled ultrasonic equipment.

The relations between ultrasonic velocities and modules are given in Eq. (5.1) and (5.2).

$$M = c_L{}^2 \cdot \rho \qquad (5.1) \qquad\qquad G = c_T{}^2 \cdot \rho \qquad (5.2)$$

The p-wave modulus M is determined by the longitudinal velocity c_L and the shear modulus G by the transversal velocity c_T. By using Eq.(3.4) and (3.6) we express Poisson´s ratio in terms of ultrasonic velocities (5.3) where R is the ratio c_L/c_T . Lamé´s constant can be obtained by a static uniaxial test at any age and remains constant during hydration. Therefore, Eq. (5.3) allows a direct determination of Poisson´s ratio simply via time of flight (TOF) measurements.

$$\nu = \frac{\lambda}{\lambda + c_L{}^2 \cdot \rho} = \frac{\lambda}{(\lambda + c_T{}^2 \cdot \rho) \cdot 2} = \frac{1}{2}\left(1 - \frac{1}{R^2 - 1}\right) \qquad (5.3)$$

TOF measurements on HCP have been performed simultaneously with buoyancy weighing of the sample. Using this technique, not only stiffening but also chemical hardening can be measured. One example is shown in Fig. 2.2 where continuous ultrasonic excitation has an accelerating effect on the reaction. In Fig. 5.1 the early reaction reduces longitudinal velocities even below ultrasonic velocity in water. This behavior is attributed to the solution process of cement in water [Pau94] and leads to values ν>0.5. From an age of 6.5 hours, longitudinal velocities increased continuously. The calculation of Poisson´s ratio happened with (5.3). Lamé´s constant has been obtained with 6.9 GPa from compression test of wet specimen after 7 days and was assumed to be constant. Fig. 5.2 shows the same result in respect to the degree of hydration.

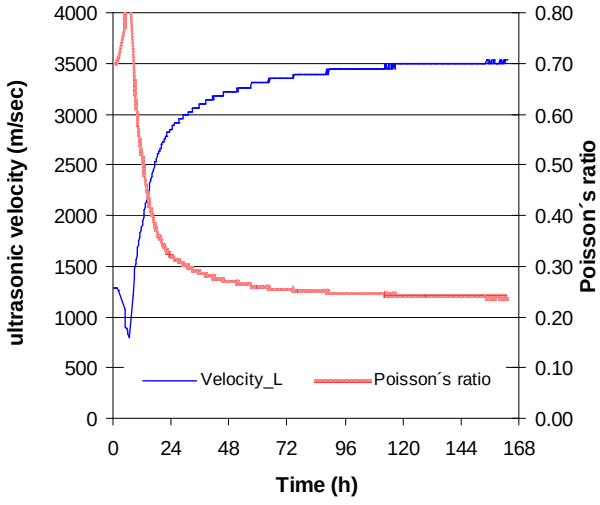

Fig. 5.1 Longitudinal velocity and Poisson´s ratio of HCP vs. reaction time.

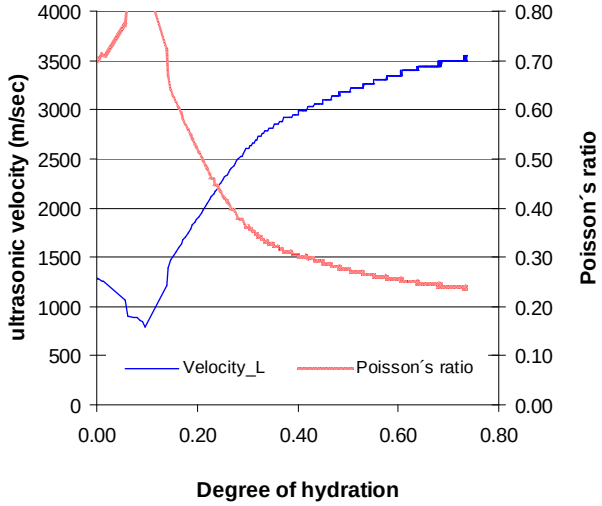

Fig. 5.2 Longitudinal velocity and Poisson´s ratio of HCP vs. degree of hydration

6 CONCLUSIONS

This paper presents a tensile strength theory for HCP and concrete, based on the chemical shrinkage volume of cement. The final volume shrinkage of cement lies between 50 to 80 cm^3/kg and is influenced by many factors. An extrapolation method of shrinkage test data has been presented to determine ultimate chemical shrinkage.

Tensile strength is defined as the specific strain work of chemical eigenstresses between reacting particles. This bond energy has been described by means of Lamé´s constant and the volume shrinkage of HCP. The strength reducing influence of porosity has been considered by a Hasselman model applied to HCP. Based on the assumption that Lamé´s constant does not change during hydration, the longitudinal ultrasonic velocity has been used to determine the declining Poisson´s ratio and the stiffness of hardening HCP. Strengthening and stiffening of HCP and concrete can be recorded simultaneously by buoyancy weighing and TOF measurements.

ACKKNOWLEDGMENT

Generous research conditions provided by the Austrian Science Act UOG 1975 are highly appreciated.

REFERENCES

[Byf80] Byfors, J.: Plain concrete at early ages, Swedish Cement Concrete Research Institute, Fo.3, (1980), ISSN 0346-6906

[Bou96] Boumiz, A., Vernet, C., Cohen Tenoudji, F.: Mechanical properties of cement pastes and mortars at early ages, Advn. Cem. Bas. Mat., (1996), 3, 94-106

[Des95] De Schutter, G., Taerwe, L.: General hydration model for Portland cement and blast furnace slag cement, Cement and Concrete Research, Vol. 25, (1995), 593-604

[Gei82] Geiker; M., Knudsen, T.: Chemical shrinkage of Portland cement pastes, Cement and Concrete Research, Vol.12, (1982), 603-610

[Nie93] Nielsen, L.F.: Strength development in hardened cement paste: examination of some empirical equations, Materials and Structures, 26 (1993), 255-260

[Pau92] Paulini, P.: A weighing method for cement hydration, Proc. of the 9th Int. Congress on the Chemistry of Cement, Vol. IV, 248-254, National Council for Cement and Building Materials, New Delhi (1992)

[Pau94] Paulini, P.: A through solution model for volume changes of cement hydration, Cement and Concrete Research, Vol.24, (1994), 488-496

[Pau10] Paulini, P.: A general strength theory based on volume shrinkage, submitted to Mechanics of Materials

[Pop90] Popovics, S; Rose, J.L.; Popovics, J.S.: The behaviour of ultrasonic pulses in concrete, Cement and Concrete Research, Vol.20, (1990), 259-270

[Pow48] Powers, T.C., Brownyard, T.L.: Studies on the physical properties of hardened Portland cement paste, PCA Bull. 22, Chicago, (1948)

[Pow58] Powers, T.C.: Structure and physical properties of hardened Portland cement paste, J. Amer. Ceramic Soc., 41, (1958), 1-6

[Sid93] Sideris, K.: The cement hydration equation, Zement-Kalk-Gips, Ed.B. 12, (1993), E337-E344

[Tap59] Taplin, J.M.: A method for following the hydration reaction in Portland cement paste, Aust. Journ. Appl. Sci., 10, (1959), 329-345

[Ver68] Verbeck, G.J, Helmuth, R.A.: Structure and physical properties of cement pastes, Proc. of the 5th Int. Congress on the Chemistry of Cement, Tokyo, (1968), Vol.III, 1-32